Supporting Information for

A series of multifunctional coordination polymers based on terpyridine and zinc halide: second harmonic generation and two-photon absorption properties and intracellular imaging

Jian Su[a,‡], Jun Zhang[a,‡], Xiaohe Tian*[,b], Meng Zhao[a], Tao Song[c], Jiancan Yu[c], Yuanjing Cui[c], Guodong Qian[c], Hong Zhong[d], Lei Luo[d], Yujin Zhang[e], Chuankui Wang[e], Shengli Li[a], Jiaxiang Yang[a], Hongping Zhou[a], Jieying Wu*[,a] & Yupeng Tian*[,a,f]

[a]Department of Chemistry, Anhui University, Hefei 230039, P. R. China.

[b]School of life science, Anhui University, Hefei 230039, P. R. China.

[c]State Key Laboratory of Silicon Materials, Cyrus Tang Center for Sensor Materials and Applications, School of Materials Science and Engineering, Zhejiang University Hangzhou 310027, China.

[d]College of Pharmaceutical Sciences, Southwest University, Chongqing 400715, P. R. China.

[e]College of Physics and Electronics, Shandong Normal University, Jinan 250014, P. R. China.

[f]State Key Laboratory of Coordination Chemistry, Nanjing University, Nanjing 210093, P. R. China.

[‡]These authors contributed equally to this work.

To whom correspondence should be addressed

E-mail: xiaohe.t@ahu.edu.cn; jywu1957@163.com; yptian@ahu.edu.cn

Table of Contents

1. Experimental Section

1.1 Materials and measurements.

All the reagents and solvents were commercially available and used as received.

FT-IR data were recorded on VERTEX 80 with KBr pellets in the 4000 – 400 cm^{-1} region. ^1H NMR spectra were recorded on 400 MHz spectrometers. Chemical shifts of **^{1}H NMR** spectra were reported in parts per million relative to tetramethylsilane (δ = 0). The following abbreviations were used to describe peak splitting patterns when appropriate: s = singlet, d = doublet, t = triplet, m = multiple. **^{13}C NMR** spectra were recorded on 101 MHz spectrometers. Chemical shifts were reported in parts per million relative to tetramethylsilane (δ = 0).

High-resolution mass spectra (HRMS) were recorded on a BRUKER VPEXII spectrometer with EI and ESI mode unless otherwise stated. **Elemental analyses (EA)** for C, H and N were performed on Vario ELIII.

TGA data were obtained on a TGA-50 (SHIMADZU) thermogravimetric analyzer with a heating rate of 10 °C min^{-1} under N_2 atmosphere. **The powder X-ray diffraction patterns (PXRD)** were collected on a XD-3 (40 kV, 40 mA) diffractometer with Cu radiation (λ= 1.54056 Å) at room temperature.

The solid state luminescence spectra were measured on an F-4500 FL spectrophotometer with the EX Slit: 2.5 nm, EM Slit: 2.5 nm and PMT Voltage: 700 V for ligand **tpatpy** and **AHU-1**, **AHU-2**, and **AHU-3**. For **time-resolved fluorescence measurements**, the fluorescence signals were collimated and focused onto the entrance slit of a monochromator with the output plane equipped with a photomultiplier tube (HORIBA HuoroMax-4P). The decays were analyzed by least-squares. The quality of the exponential fits was evaluated by the goodness of fit (χ^2). The **fluorescent quantum yield** of solid samples were measured with integrating sphere.

The **second-order nonlinear optical intensity** was estimated by measuring a powder sample 63 - 90 μm in diameter relative to **Urea**. A pulsed Q-switched Nd:YAG laser at a wavelength of 1064 nm was used to generate second-order harmonic generation (SHG signals). The backscattered SHG light of 532 nm was collected and detected with a photomultiplier through a monochromator. The **two-photon emission fluorescence** (TPEF) spectra were measured at femtosecond laser pulse and Ti: sapphire system (680–1080 nm, 80 MHz, 140 fs) as the light source.

The morphologies of the nanoparticles were obtained on a **transmission electron microscope (TEM**, JEM-2100) and a field-emission scanning electron microscope (FESEM, Hitachi S-4800). The Dynamic Light Scattering (DLS) measurements were conducted on a Particle Size Analyzer (Nano ZS90, Malvern Instruments, UK) at a temperature of 25 °C.

Micro-scale and nanoscale samples and mice liver were luminescently imaged on a Zeiss LSM 710 META upright **confocal laser scanning microscope** using magnification 40× and 100× oil-dipping lenses for mono-layer cell cultures. Image data acquisition and processing was per-formed using Zeiss LSM Image Browser, Zeiss LSM Image Expert and Image J.

Single-crystal X-ray Structure Studies. Single-crystal X-ray crystallographic studies: Data were collected on a Bruker Smart APEX II diffractometer with a CCD area detector. Raw data collection and reduction were done using APEX2 software. [1] Adsorption corrections were applied using the SADABS routine. The structures were solved by direct methods and refined by full-matrix least-squares on F^2 using the SHELXTL software package.[2] Non-hydrogen atoms were refined with anisotropic displacement parameters during the final cycles. Hydrogen atoms of **tpatpy** were calculated in ideal positions with isotropic displacement parameters. The X-ray crystallographic coordinates for structures reported in this Article have been deposited at the Cambridge Crystallographic Data Centre (CCDC), under deposition number CCDC 1440286-1440289 These data can be obtained free of charge from the Cambridge Crystallographic Data Centre via www.ccdc.cam.ac.uk/data_request/cif.

1.2 Synthesis

The **tpatpy** ligand was prepared by the Vilsmeier-Haack reaction with 4-(diphenylamino)benzaldehyde as raw material (**Figure S1** and **Scheme S1**). **AHU-1** to **AHU-3** were assembled by tardily reacting **tpatpy** and ZnX_2 (X= Cl, Br and I) (1:1 molar ratio) which absolutely dissolved in $CHCl_3$ and CH_3OH, respectively, at room temperature for about one week. The reaction produced needle-like yellow crystals. The phase purity of **AHU-1** to **AHU-3** was confirmed by infrared spectroscopy, powder X-ray diffraction (PXRD) analysis (See **Figure S2** and **Figure S3**) and elemental analysis (EA).

1.2.1 Synthesis of tpatpy

4-Acetylpyridine (2.67 g, 22.00 mmol) was added to a solution of 4-formyltriphenylamine (2.73 g, 10.00 mmol) in EtOH (50 mL). 5 mL cooled KOH (1.71 g, 30.00 mmol) aqoeous solution were then added followed by aqueous NH_3 (25%, 30 mL) and the resulting solution was stirred at 85 °C for 24 h (See Supplementary **Figure S1** and **Scheme S1**). The **tpatpy** was obtained as a light-yellow solid (2.70 g 5.67 mmol). Yield 56.70 %. Melting point: 248 ~ 249°C. ^{1}H NMR (400 MHz, $CDCl_3$) δ 8.11−8.10 (d, 2H), 8.02 (s, 1H), 7.63−7.61 (d, 1H), 7.34−7.31 (t, 2H), 7.21−7.17 (m, 3H), 7.13−7.10 (t, 1H); ^{13}C NMR (400 MHz, $CDCl_3$) δ 154.28, 153.37, 151.13, 147.52, 145.43, 144.28, 132.31, 130.01, 129.80, 126.27, 125.65, 124.88, 121.98 and 119.49. HR-MS (ESI) m/z calcd for $C_{33}H_{24}N_4$ [MH^+] 477.2079, found 477.2086.

1.2.2 Synthesis of AHU-1 to AHU-3

AHU-1: $[Zn(tpatpy)Cl_2•(H_2O)]_n$ To the solution of **tpatpy** (0.0476 g, 0.010 mmol) in 6 mL $CHCl_3$ and 1 mL CH_3OH, was carefully added 3 mL CH_3OH then carefully layered 10 mL methanolic solution of $ZnCl_2$ (0.0136 g, 0.010 mmol) in a test tube. The tube was sealed and left standing at room

temperature for several days during which time X-ray quality, yellow needle-like crystals grew. These were collected by filtration, washed with $CHCl_3$ and dried in air (51.4 mg, 81.6%, calc. based on **tpatpy**). Calcd for $C_{33}H_{26}OZnN_4$ (Mr= 630.87): C, 62.83; H, 4.154; N, 8.881 %. Found: C, 63.23; H, 4.017; N, 9.029 %. FT-IR (KBr pellet, cm^{-1}): 516.3(w), 651.2(w), 698.2(w), 758.2(w), 833.9(w), 1025.2(w), 1065.1(w), 1201.2(w), 1330.4(w), 1404.2(w), 1428.8(s), 1489.2(s), 1588.0(w), 1617.6(w), 177.1(w).

AHU-2: $[Zn(tpatpy)Br_2\bullet(H_2O)]_n$ The procedure was as for **AHU-1**, starting with methanolic solution of $ZnBr_2$ (0.0225 g, 0.010 mmol). Yellow needle-like crystals were collected by filtration, washed with $CHCl_3$ and dried in air (59.8 mg, 83.2%, calc. based on **tpatpy**). Calcd for $C_{33}H_{26}Br_2OZnN_4$ (Mr= 719.77): C, 55.31; H, 3.660; N, 7.823 %. Found: C, 55.36; H, 3.473; N, 7.970 %. FT-IR (KBr pellet, cm^{-1}): 516.3(w), 651.2(w), 698.2(w), 758.2(w), 833.9(w), 1025.2(w), 1065.1(w), 1201.2(w), 1330.4(w), 1404.2(w), 1428.8(s), 1489.2(s), 1588.0(w), 1617.6(w), 177.1(w).

AHU-3: $[Zn(tpatpy)I_2]_n$ The procedure was as for **AHU-1**, starting with methanolic solution of ZnI_2 (0.0319 g, 0.010 mmol). Yellow needle-like crystals were collected by filtration, washed with $CHCl_3$ and dried in air (63.4 mg, 79.7%, calc. based on **tpatpy**). Calcd for $C_{33}H_{24}I_2Zn$ (Mr= 795.75): C, 49.88; H, 3.05; N, 7.055 %. Found: 49.88; H, 3.08; N, 6.970 %. FT-IR (KBr pellet, cm^{-1}): 516.3(w), 651.2(w), 698.2(w), 758.2(w), 833.9(s), 1025.2(w), 1065.1(w), 1201.2(w), 1328.1(w), 1404.2(w), 1428.8(s), 1489.2(s), 1588.0(w), 1617.6(w), 177.1(w).

1.2.3 Synthesis of micro-scale and nano-scale AHU-1

The micro-scale **AHU-1** was synthesis in a 35 mm × 10 mm style cell culture Dish. 40 μL 5×10^{-4} mol/L $ZnCl_2$ was cover with 40 μL 5×10^{-4} mol/L **tpatpy**, then standing several minutes.

The nano-scale **AHU-1** was synthesis in a 10 mL centrifuge tube with ultrasonic cleaners. In the ultrasonic environment, 4 mL 5×10^{-4} mol/L $ZnCl_2$ solution was dropwisely added into 4 mL 5×10^{-4} mol/L tpatpy solution, and intense rock, 10 minutes later standing several minutes. The liquid supernatant was pick out for biological imaging with the average size of 13 nm.

1.2.4 Synthesis of PEG_{2000}-PLA_{2000} grafted nano-scale AHU-1

The nanoscaled **AHU-1** was synthesis like the procedure in **1.2.3**. In the ultrasonic environment, 20 mg PEG_{2000}-PLA_{2000} and 1 mL CH_3CN was added in a 5 mL centrifuge tube, after 30 min, 40 μL solution of nanoscaled **AHU-1** was added and keep about 30 min. Then, the solvent was evaporated under reduced pressure and 10 mL PBS (Phosphate Buffer Solution) buffer was added to the resultant residue. The solution was put in a sonic bath for 3 hours. The result PEG_{2000}-PLA_{2000} grafted nanoscaled **AHU-1** solution was obtained through a 0.22 μm filter.

1.3 Methods to deal with the liver tissues

Mouse was terminally anaesthetised and transcardially perfused with phosphate buffered saline (PBS) 0.1M pH 7.4. The frist fixation was performed in 4% paraformaldehyde solution, then the mixture of $CHCl_3$ and CH_3OH perfuse. Their liver was extracted and perfused with the solution of nanoscaled **AHU-1**, the perfused liver block then sectioned into 20 μm in the sagittal plane using a cryostat (Leica 1900). Sections were mounted cover-slipped using an aqueous Prolong Diamond Antifade medium (Life Technology P36970), and imaged directly using a Zeiss LSM 710 confocal system using 20 x, 63 x and 100 x magnification IR Zeiss dipping (oil) objective.

1.4 Cytotoxicity study

HepG2 cells and HELF cells growing in the log phase were seeded into 96-well plates (~ 1×104 cells/well) and allowed to adhere for 24h. PEG_{2000}-PLA_{2000} grafted nanoscaled **AHU-1** stock solutions were diluted by fresh mediumin to desired concentration (~5, ~10, ~20, ~40, ~60 μM). The cell medium was then exchanged by different concentrations of **AHU-1** medium solutions. They were then incubated at 37 °C in 5% CO_2 for 24 h before cell viability was measured by the MTT assay. The cell medium solutions were exchanged by 100 μL of fresh medium, followed by the addition of 10 μL (5 mg / mL) MTT solution to each well. The cell plates were then incubated at 37 °C in 5% CO_2 for 4 h. Absorbance was measured at 450 nm. The absorbance measured for an untreated cell population under the same experimental conditions was used as the reference point to establish 100% cell viability. Duplicated experiments have been tested.

1.5 Cell culture and imaging

For HepG2 cells (liver hepatocellular carcinoma, ATCC No. HB-8065), the medium used was Dulbecco's modified Eagle's medium (DMEM) supplemented with 10% fetal calf serum (FCS, GIBCO), penicillin and streptomycin, L-glutamine and fungizone. For live cell confocal laser scanning microscopy experiment, HepG2 cells were seeded in 24-well glass bottom plate (In Vitro Scientific, P24-1.5H-N) at density of 10,000, and incubated for 72 - 96 hours at 37 °C in 95% air 5% CO_2 in order to allow the cells to reach ~90% confluence, the medium changed every two days. 20 μL of PEG_{2000}-PLA_{2000} grafted nanoscaled **AHU-1** solution was added to the culture medium for 30 min at 37 °C in 95% air 5% CO_2 and then imaged with confocal microscopy.

2. Crystal structure of tpatpy

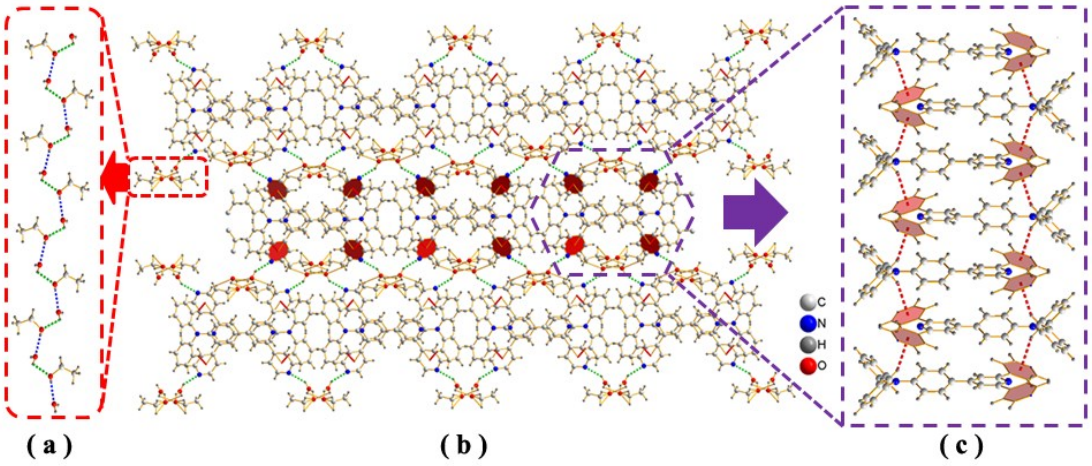

Figure S1. Crystal structure of **tpatpy**. (a) The ethanol-water one-dimentional chain constructed by the hydrogen bonds O-H···O. (b) The three-dimentional stacking of **tpapty** crystal structure. (c) The one-dimentional chain-like structure of **tpatpy** constructed by the C-H···π stacking.

3. Comparison of Infrared spectra

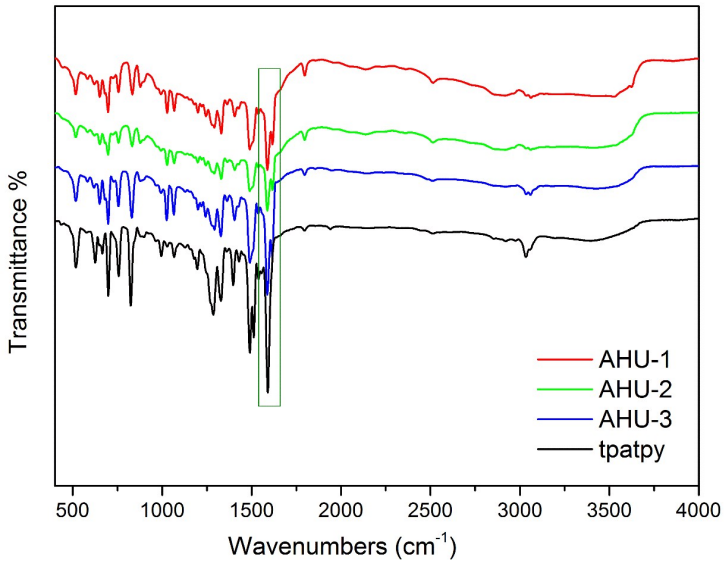

Figure S2. Infrared spectra of **tpatpy**, **AHU-1**, **AHU-2** and **AHU-3**. The special peak of pyridine at around 1591 cm^{-1} of free tpatpy molecule have divided into two peaks at 1588 cm^{-1} and 1615 cm^{-1} in the spectra of **AHU-1**, **AHU-2** and **AHU-3**.

4. Comparison of Powder XRD patterns

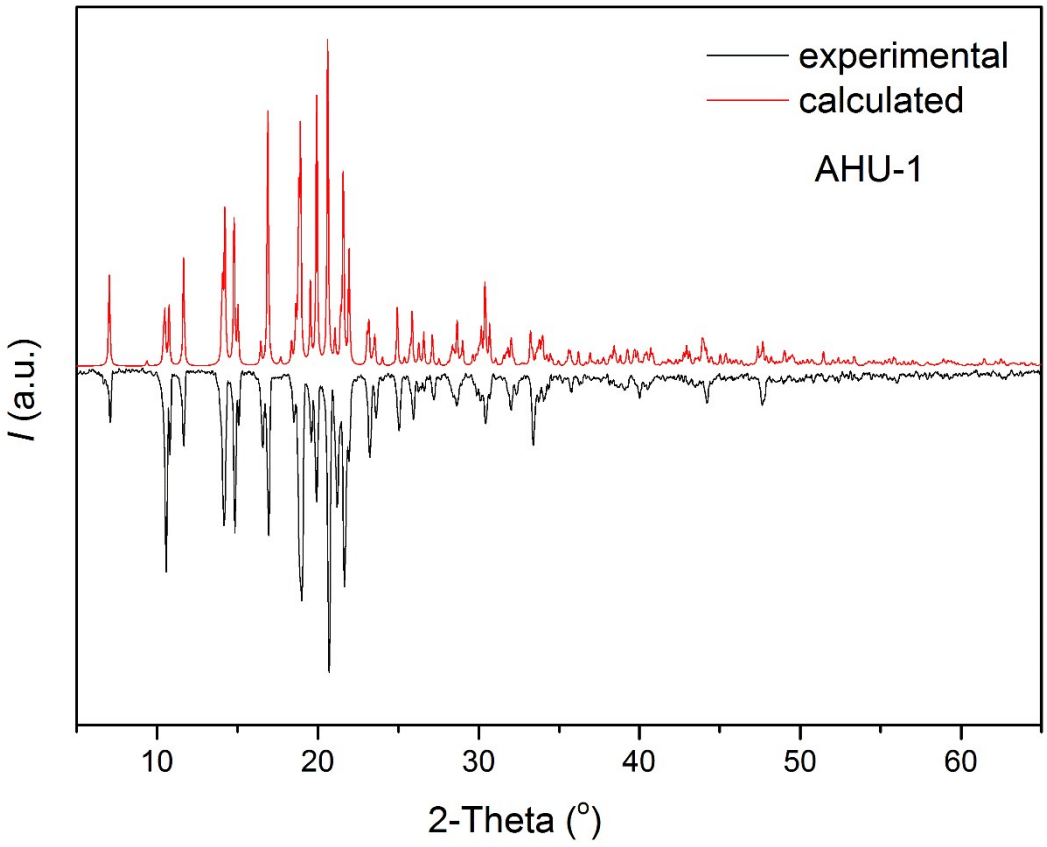

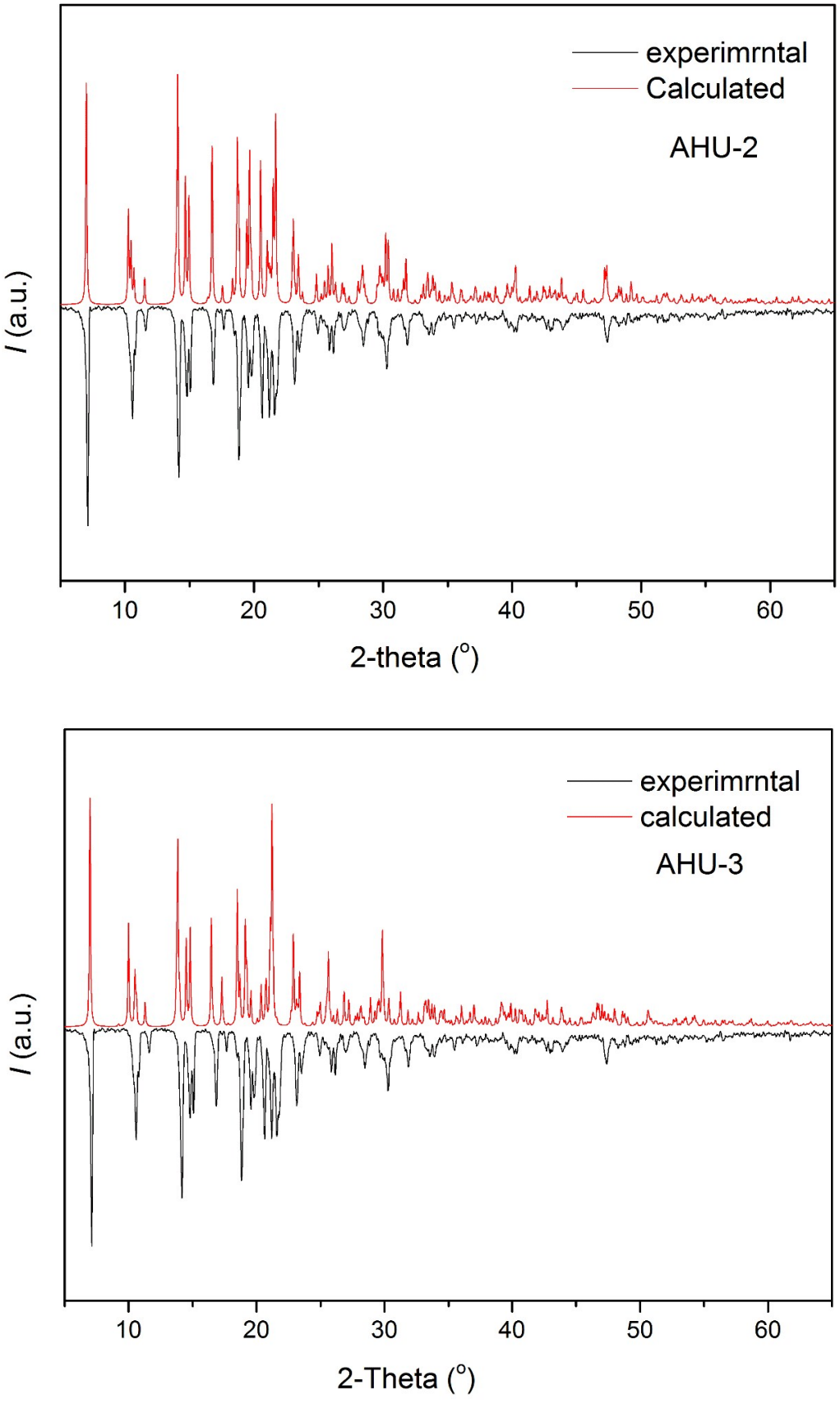

Figure S3. Powder XRD patterns of the products **AHU-1**, **AHU-2** and **AHU-3** obtained from the experiment associated with the simulated XRD pattern from the single crystal X-ray data.

5. Crystal Structures of AHU-2 and AHU-3

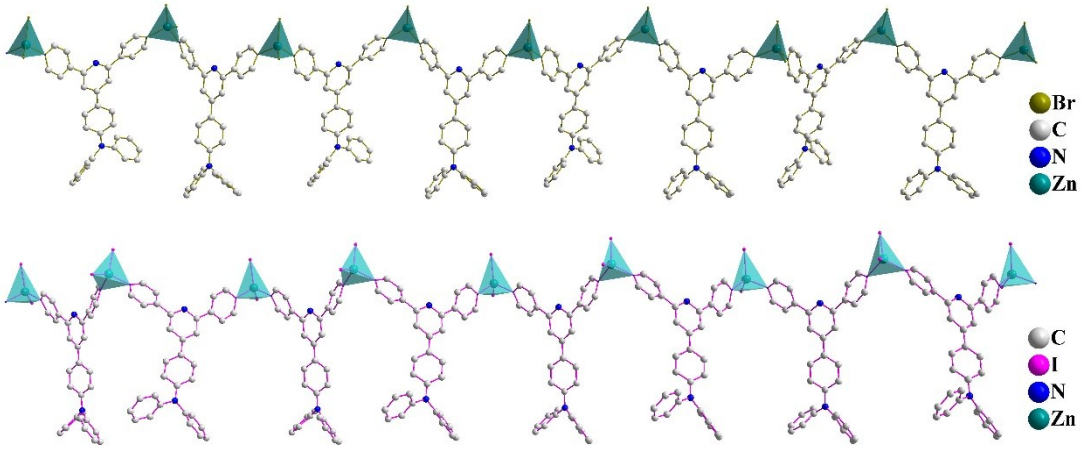

Figure S4. The one-dimentional chain-like structures of **AHU-2** and **AHU-3**.

6. Asymmetric unit of AHU-1, AHU-2 and AHU-3

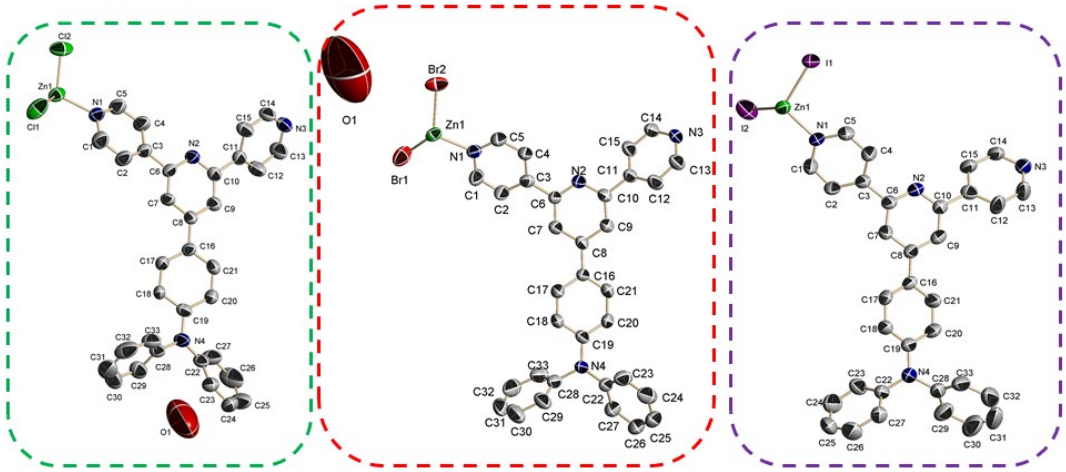

Figure S5. The asymmetric unit of **AHU-1**, **AHU-2** and **AHU-3**. Displacement ellipsoids are drawn at the 50% probability level. Hydrogens are omitted for clarity.

7. Comparison of TGA plots

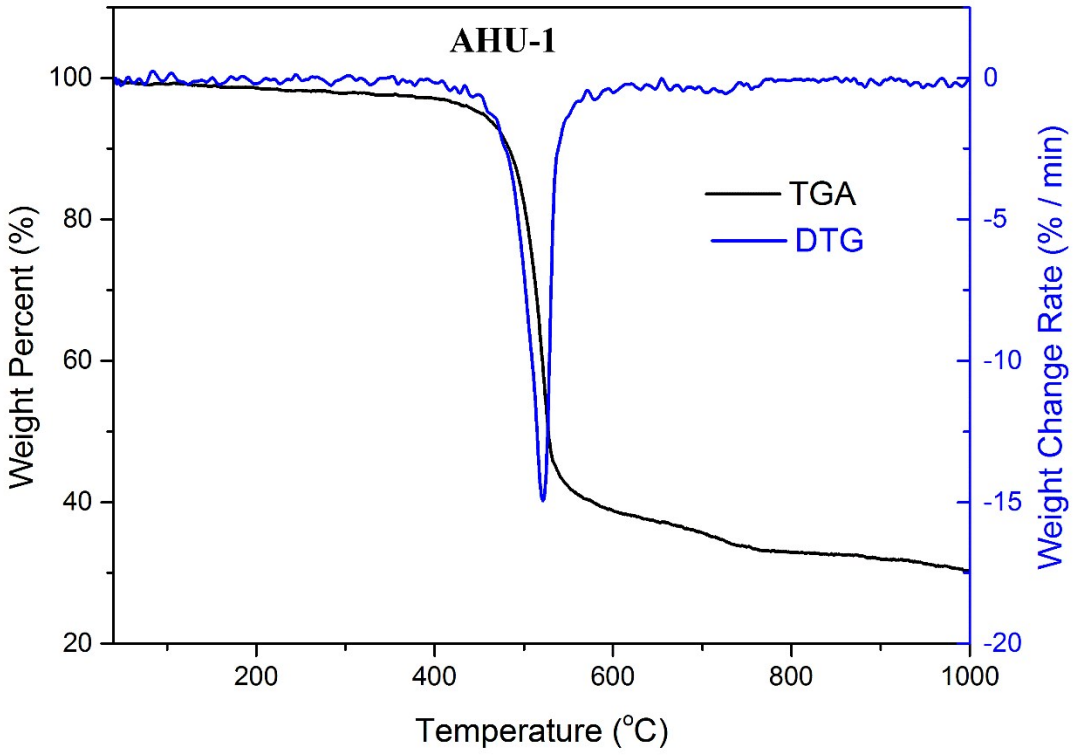
AHU-1
TGA
DTG
Weight Percent (%)
Weight Change Rate (% / min)
Temperature (°C)
100
80
60
40
20
0
-5
-10
-15
-20
200
400
600
800
1000

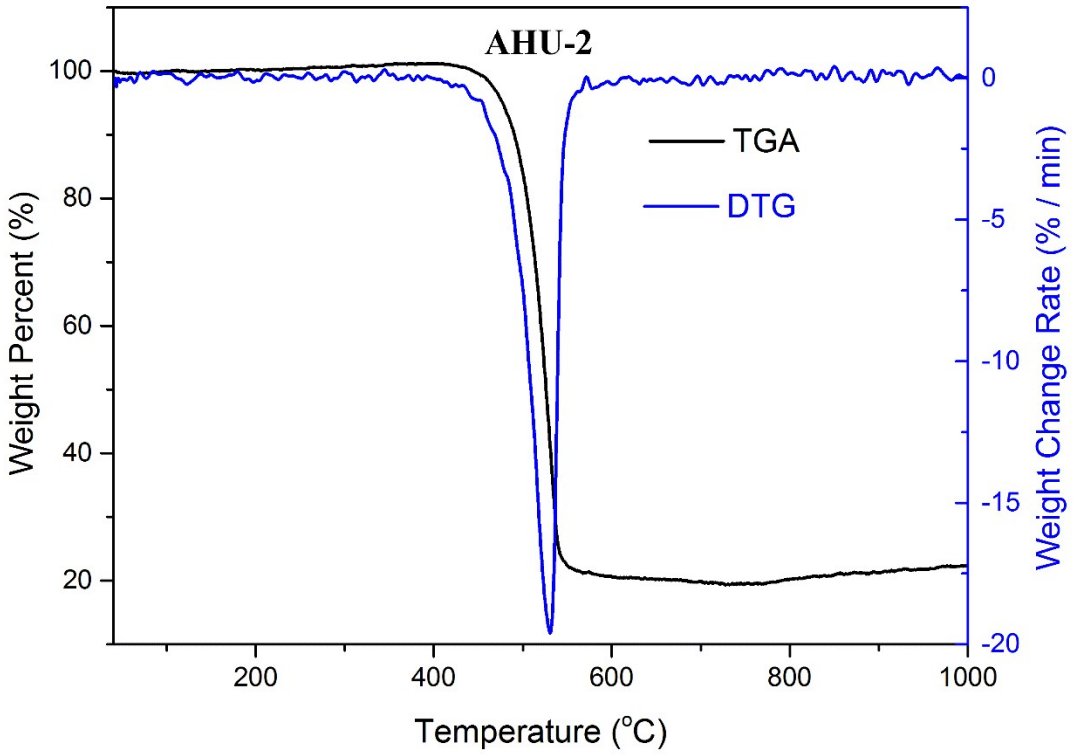
AHU-2
TGA
DTG
Weight Percent (%)
Weight Change Rate (% / min)
Temperature (°C)
100
80
60
40
20
0
-5
-10
-15
-20
200
400
600
800
1000

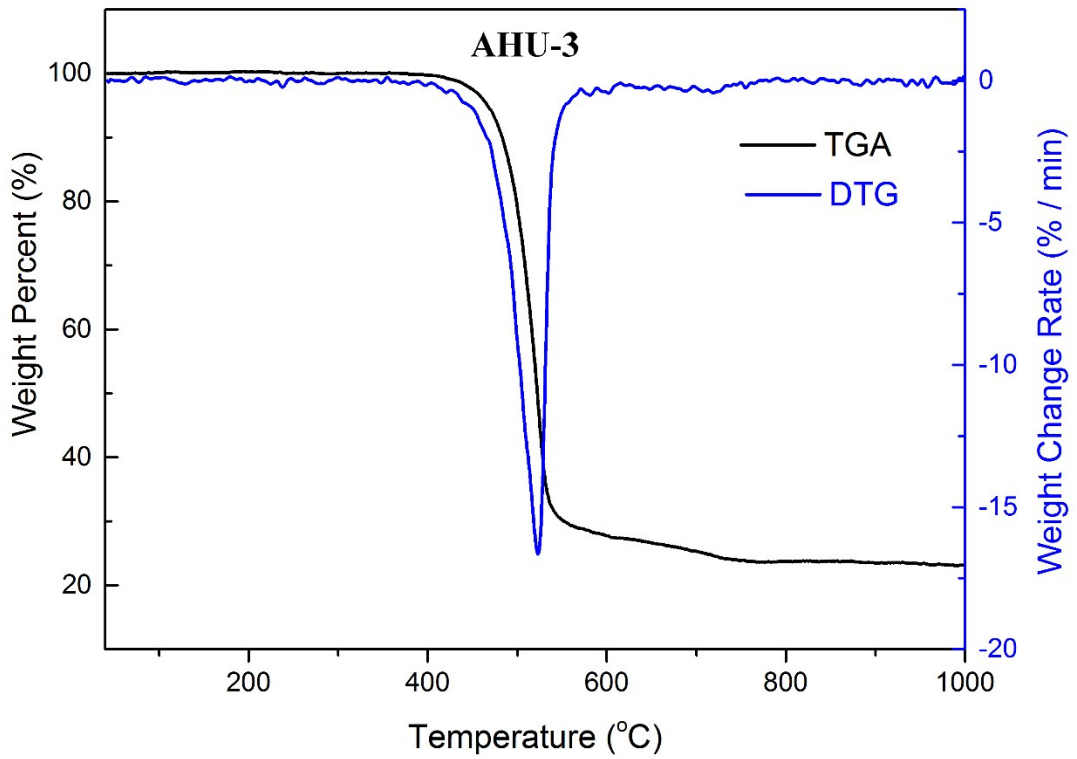

Figure S6. The TGA (black line) and DTG (blue line) plots of **AHU-1**, **AHU-2** and **AHU-3**.

8. Time-resolved fluorescence curves

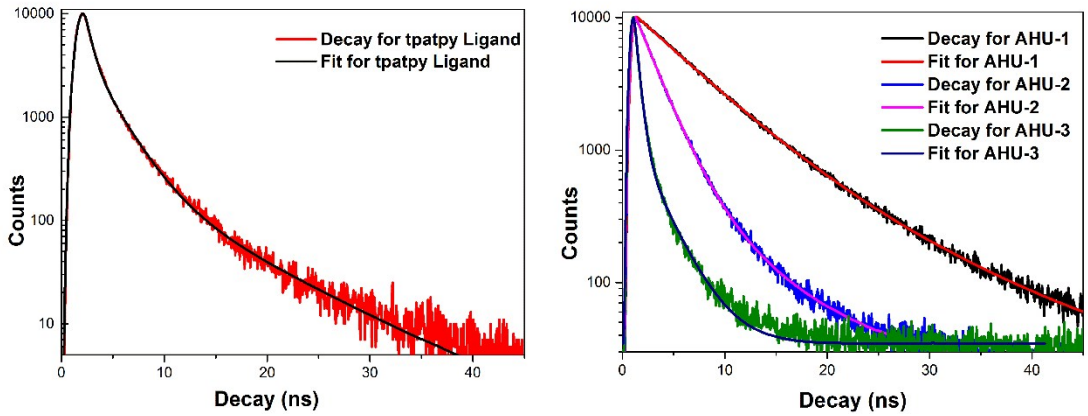

Figure S7. Luminescenes decay curve of **tpatpy** and **AHU-1** to **AHU-3** in the solid state at room temperature with the fluorescence lifetimes1.14, 13.15, 4.80, and 1.14 ns, respectively.

9. Linear and nonlinear optical properties of tpatpy

10.1 Linear and nonlinear optical properties of tpatpy in solution

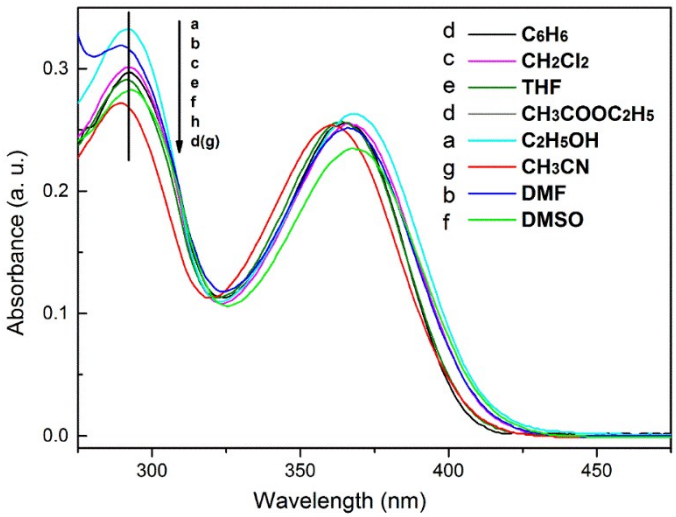

Figure S8. Absorption spectra of ligand **tpatpy** in different solvents with the centration of 1 × 10^{-5} M at room temperature.

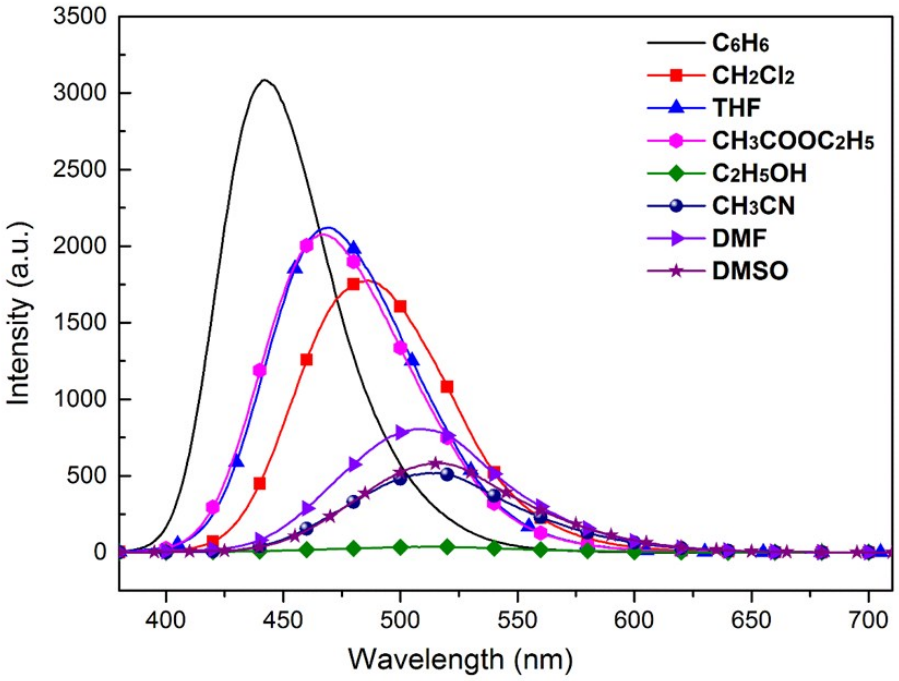

Figure S9. Time-resolved fluorescence curves of ligand **tpatpy** in different solvents with the centration of 1 × 10^{-5} M at room temperature.

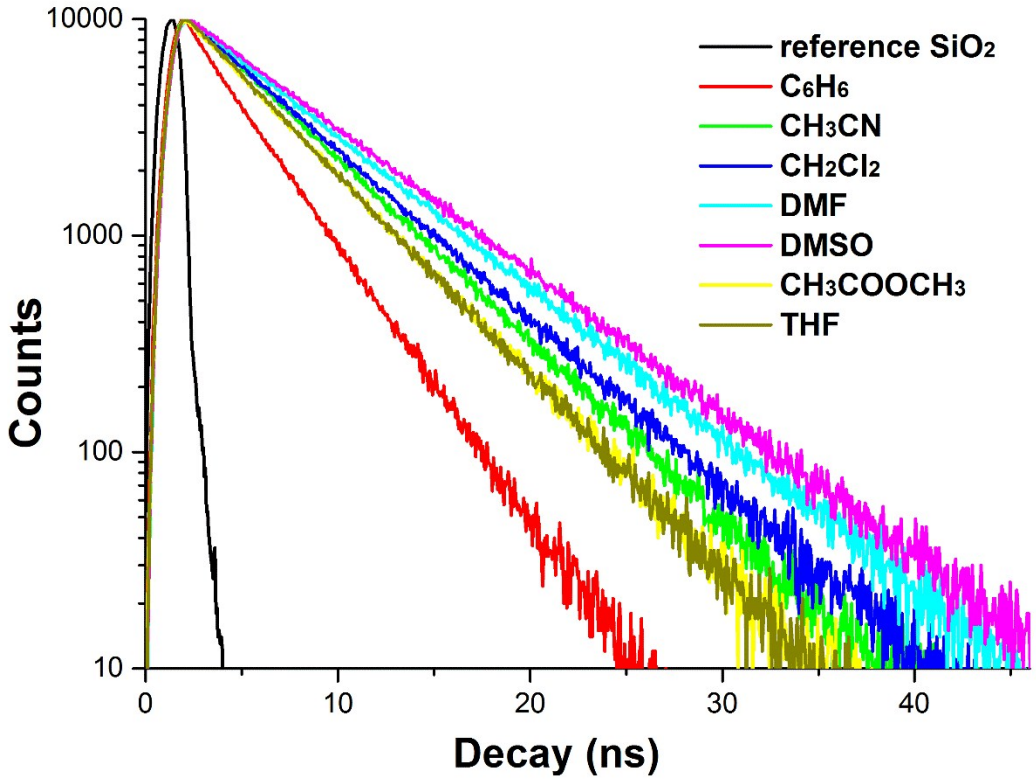

Figure S10. Luminescenes decay curve of ligand **tpatpy** in different solvents with the centration of 1 × 10^{-5} M at room temperature.

The fluorescent quantum yield of ligand **tpatpy** in different solvents were measured with comparative method.[3] The standard sample is Quinine sulfate in the solution of 0.1 M H_2SO_4. The Quinine sulfate and tpatpy are in the centration of 1 × 10^{-5} M at room temperature. Absolute values are calculated using the standard samples which have a fixed and known fluorescence quantum yield value, according to the following equation:

$$\Phi_s = \Phi_r\left(\frac{A_r\eta_s^2 D_s}{A_s\eta_r^2 D_r}\right)$$

Where the subscripts ***r*** (reference) and ***s*** (sample) denote standard and test respectively, **Φ** is the fluorescence quantum yield, **D** is the integrated fluorescence intensity, **A** is the absorbance, and **η** the refractive index of the solvent.

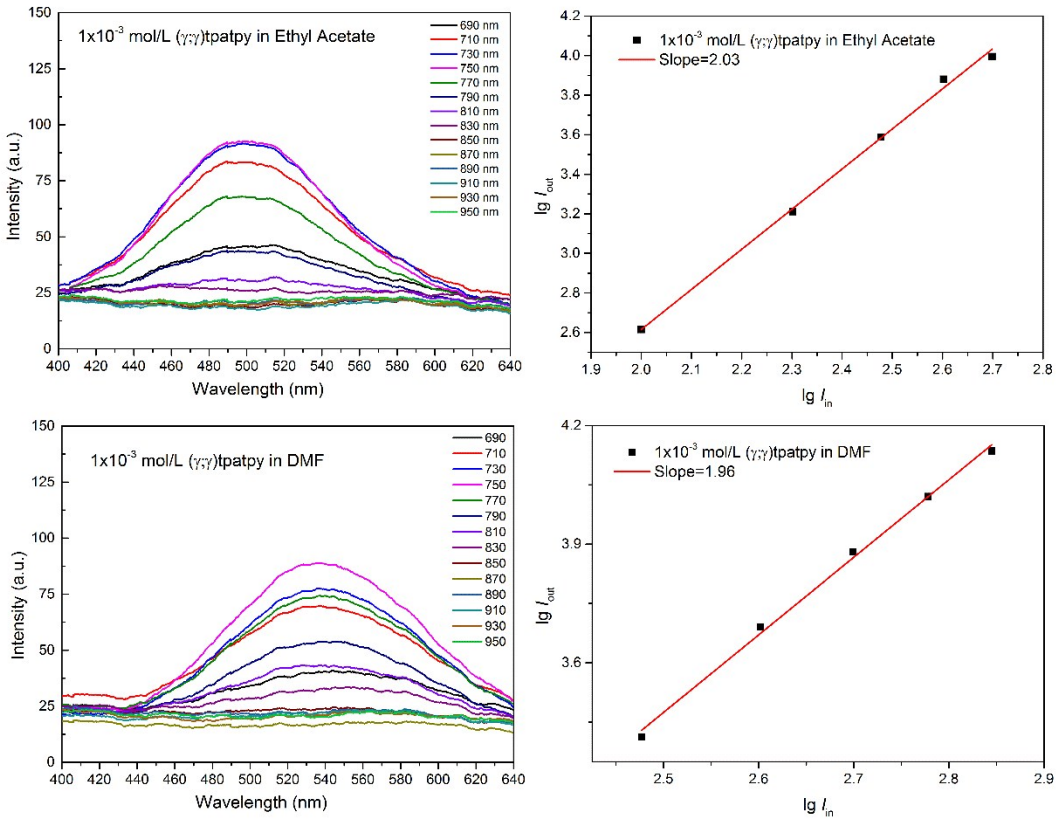

Figure S11. TPEF measurements of **tpatpy** in solution. TPEF measurements of 1.0 × 10^{-3} mol/L **tpatpy** ligand in DMF and ethyl acetate under excited at 500 mV with different λ_{ex}. Output fluorescence (lgI_{out}) vs. the square of input laser powder (lgI_{out}) for 1.0 × 10^{-3} mol/L **tpatpy** ligand in DMF and ethyl acetate carried out at 750 nm.

The two-photon excitation cross sections was determined by comparing their TPEF to that of fluorescein (fluorescein was in the aqueous solution of 0.1 M NaOH), according to the following equation: [4]

$$\delta = \delta_{ref}\frac{\Phi_{ref}c_{ref}n_{ref}\ \ F}{\Phi\ \ \ c\ \ \ n\ \ F_{ref}}$$

Where the subscripts ***ref*** (reference) denote standard, fluorescein in an aqueous solution of NaOH (pH = ~11) was used as reference and samples were all at aconcentration of 1.0 × 10^{-3} mol L^{-1} with a 1 cm standard quartz cell. ***F*** is the two-photon excited fluorescence integral intensity of the solution emitted at the exciting wavelength. **Φ**, **n** and **c** are the quantum yield of the fluorescence, the refractive index of the solvent, and the concentration of the solution, respectively. The values of $\boldsymbol{\delta_{ref}}$ at different wavelengths and $\boldsymbol{F_{ref}}$ are taken from the literature. [3,5]

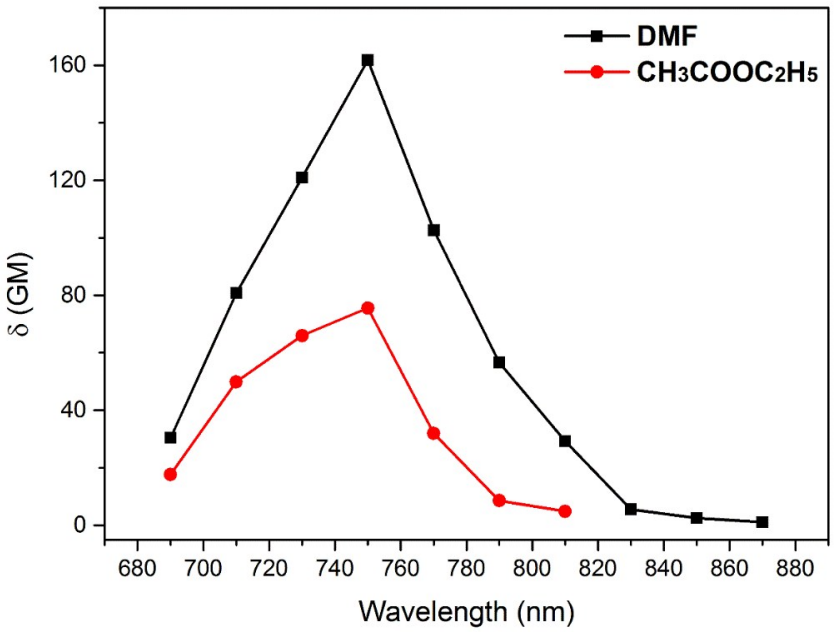

Figure S12. Two photon absorption cross-sections of **tpatpy** in $CH_3COOC_2H_5$ and DMF vs. excitation wavelengths of identical energy of 500 mW.

10. TPEF measurements of AHU-1 in crystal

The TPEF intensity of **AHU-1** shown in Figure 3 maybe not the optimal λ_{ex}. But, the laser with shorter wavelength (below 720 nm) will damage the crystal of **AHU-1**, due to its high energy. In order to keep the same experimental conditions, FL data below 720 nm were fail to collect.

11.1 Stability of AHU-1 to AHU-3 in the solvent of DMF

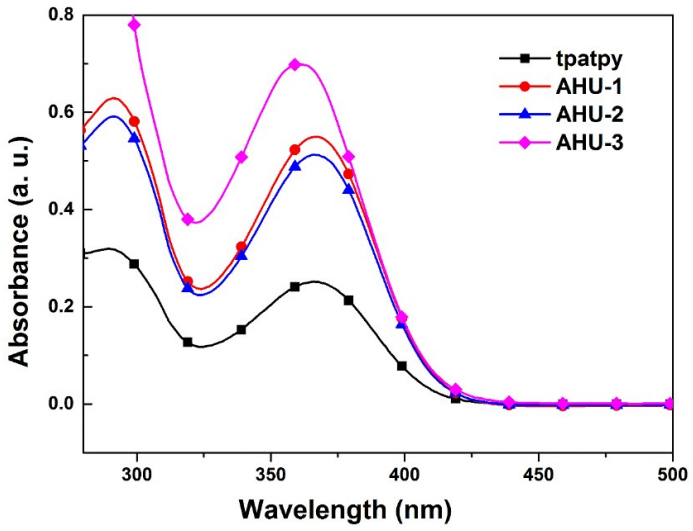

Figure S13. Absorption spectra of ligand **tpatpy**, **AHU-1**, **AHU-2** and **AHU-3** in DMF with the centration of 1×10^{-5} mol/L at room temperature.

11.2 Calculation of two-photon action cross-sections

As shown in the article of Nature Communications (doi: 10.1038/ncomms8954)[6], two-photon action cross-sections of the our samples at 800 nm can be obtained frome the ratio of the measured PL strengths from the perylene to the samples ($F_{2(Py)}/F_{2(X)}$)=[$(\eta\sigma_2)_{Py}\cdot\rho_{Py}\cdot(I_{00}^2)_{Py}$]/ [$(\eta\sigma_2)_X\cdot\rho_X\cdot(I_{00}^2)_X$]

where $F_{2(Py)}$ and $F_{2(X)}$ are the measured PL strengths.

Take ligand **tpatpy** as a standard sample, the $\eta\sigma_2$ of **AHU-1** were determined.

$$\frac{F_{2(L)}}{F_{2(CP)}} = \frac{(\eta\sigma_2)_L}{(\eta\sigma_2)_{CP}} \frac{\rho_L}{\rho_{CP}} \frac{(I_{00}^2)_L}{(I_{00}^2)_{CP}}$$

L, Ligand; CP, coordination Polymer; F_2 is the measured PL strengths; η is the fluorescent quantum yield; ρ is the sample molar concentration; σ_2 is the two-photon absorption cross-section; I_{00} is the peak intensity of the input laser pulse at the focal point.

Under the same excited energy of 500 mW, $(I_{00}^2)_L = (I_{00}^2)_{CP}$. $\rho_L = 1\times10^{-3}$ mol/L = 1×10^{-6} mol·cm^{-3}; ρ_{CP} = [1.383 (g·cm^{-3})] / [630.87 (g/mol)]= 22×10^{-4} mol·cm^{-3}. $\eta_{(L)}$ = 0.71.

Table S1. The parameters of $\sigma_{2(L)}$, $F_{2(L)}$ and $F_{2(CP)}$.

Wavelength (nm)	$\sigma_{2(L)}$	$F_{2(L)}$	$F_{2(CP)}$
730	66.97	77.5	3510
750	75.58	88.9	2490
770	31.96	73.8	2129
790	8.58	53.6	1699
810	4.87	43.5	1619

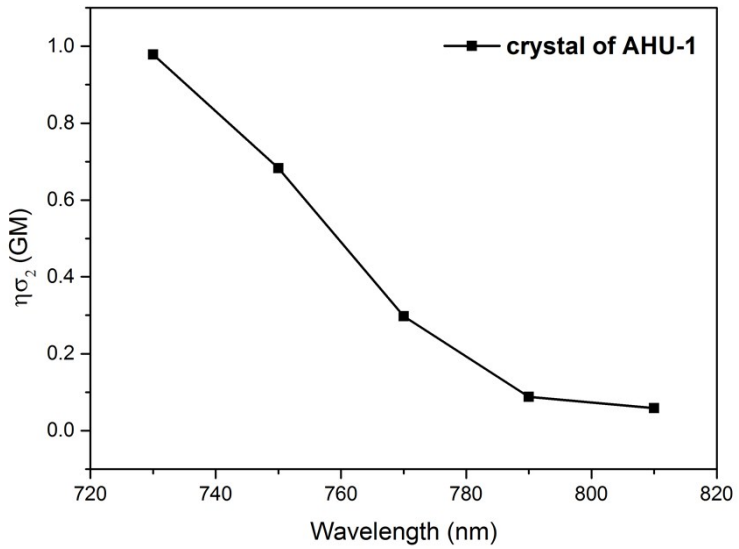

Figure S14. Two photon action cross-sections of **AHU-1** in Crystal.

11. SHG measurements in different size

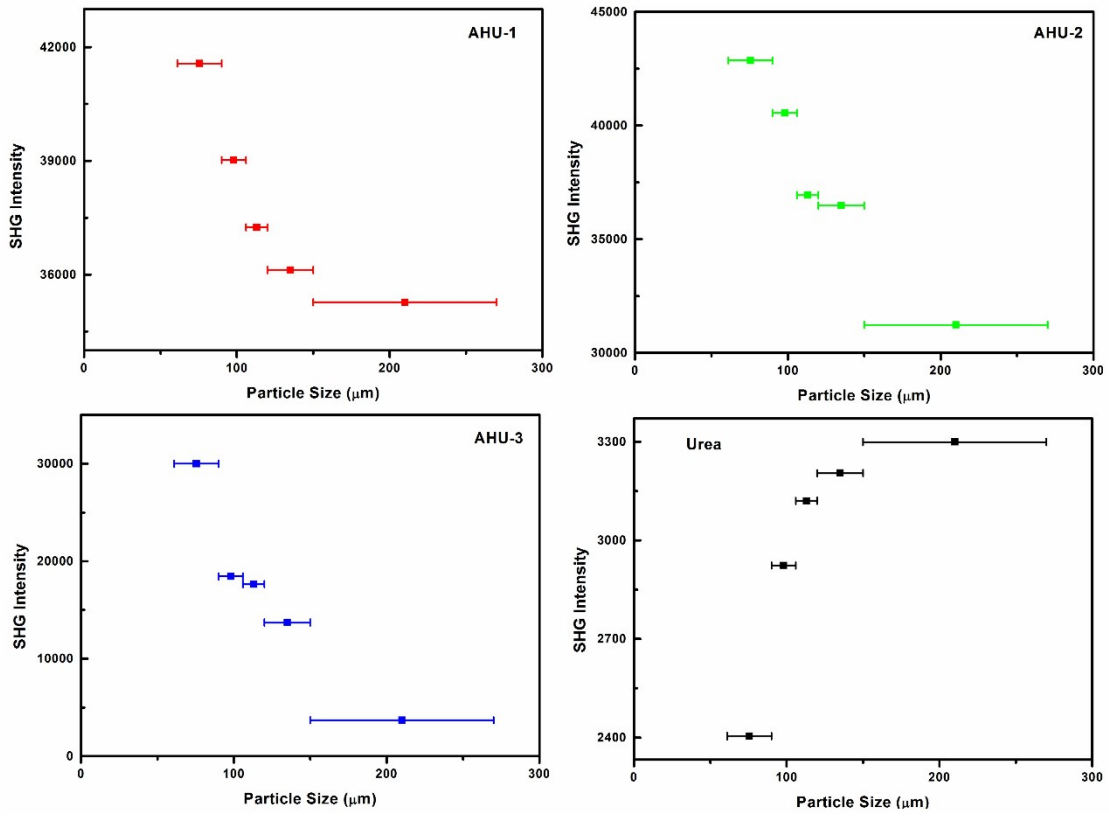

Figure S15. SHG measurements of **Urea**, **AHU-1**, **AHU-2** and **AHU-3** at the given sizes 61 - 90, 90 - 106, 106 - 120, 120 - 150 and 150 - 270 μm.

12. Description of DFT calculation

The DFT calculation of tpatpy, AHU-1, AHU-2 and AHU-3.

All calculations were performed with the Gaussian 09 software package.[7] To better understand the charge transfer state, time-dependent density functional theory (TD-DFT) calculations on all the compounds were carried out in vacuum. Optimizations were carried out with B3LYP functional without any symmetry restraint, and the TD-DFT calculations were performed on the optimized structure with Lee–Yang–Parr functional (B3LYP) functional.[8] Geometry optimization of the singlet ground state and the TD-DFT calculation of the lowest 25 singlet–singlet excitation energies were calculated with a basis set composed of 6–31 G* for C H N atoms and the Lanl2dz basis set for Zn, Cl, Br and I atoms were downloaded from the EMSL basis set library. An analytical frequency confirms evidence that the calculated species represents a true minimum with-out imaginary frequencies on the respective potential energy surface. With the optimized structure, we calculated the vector component of molecular hyperpolarizability the along the dipole moment direction through Polar calculation.

13. Charge transfer pictures

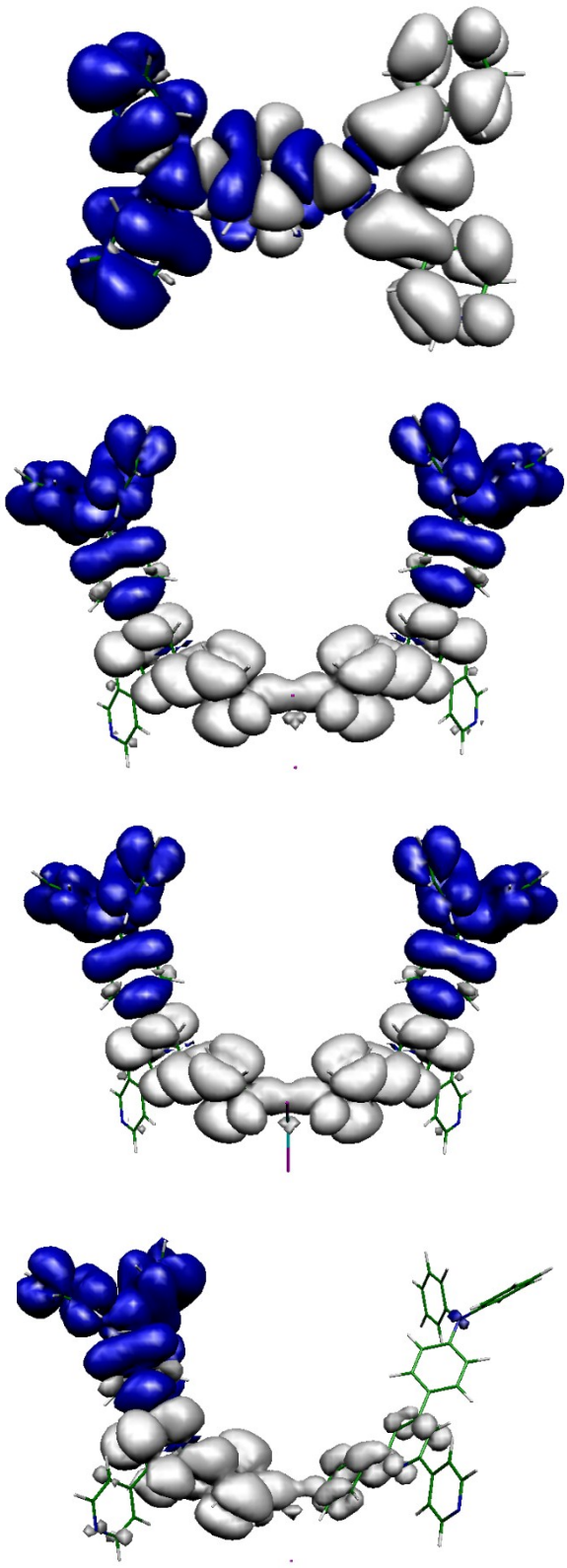

Figure S16. Charge transfer between the charge transfer (CT) states and the ground state of the compounds **tpatpy**, **AHU-1**, **AHU-2** and **AHU-3**, respectively. The gray and blue colors indicate electron density increase and decrease, respectively.

14. TEM images of the nanoscaled AHU-1

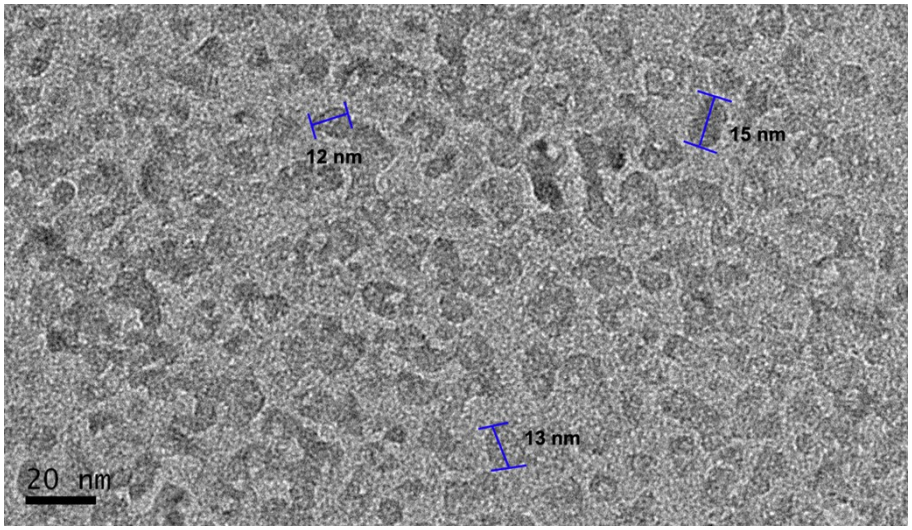

Figure S17. TEM images of the nanoscaled **AHU-1**.

15. SEM images and hydrodynamic size distribution of $mPEG_{2000}$-PLA_{2000} grafted AHU-1

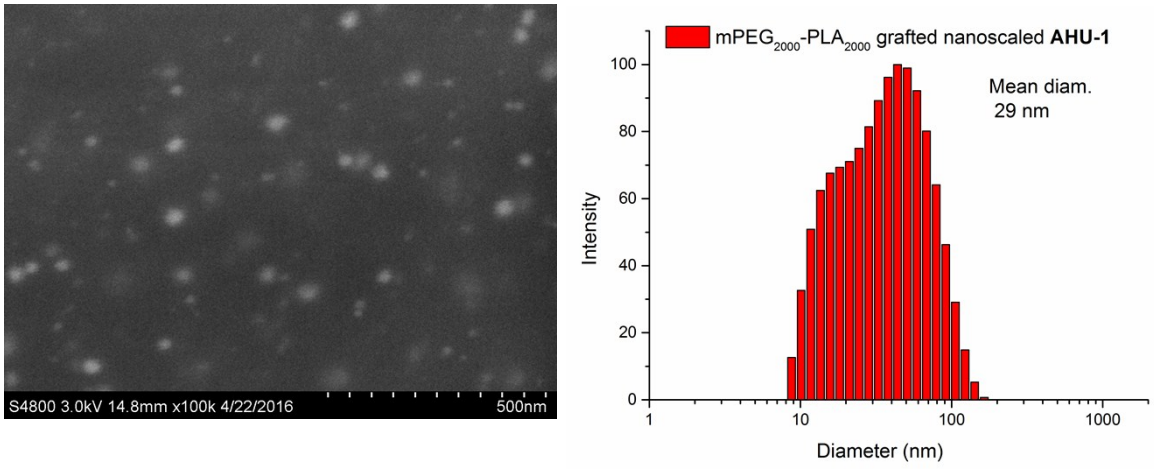

Figure S18. SEM images and hydrodynamic size distribution of the nanoscaled $mPEG_{2000}$-PLA_{2000} grafted **AHU-1**.

16. Cytotoxicity study of $mPEG_{2000}$-PLA_{2000} grafted AHU-1

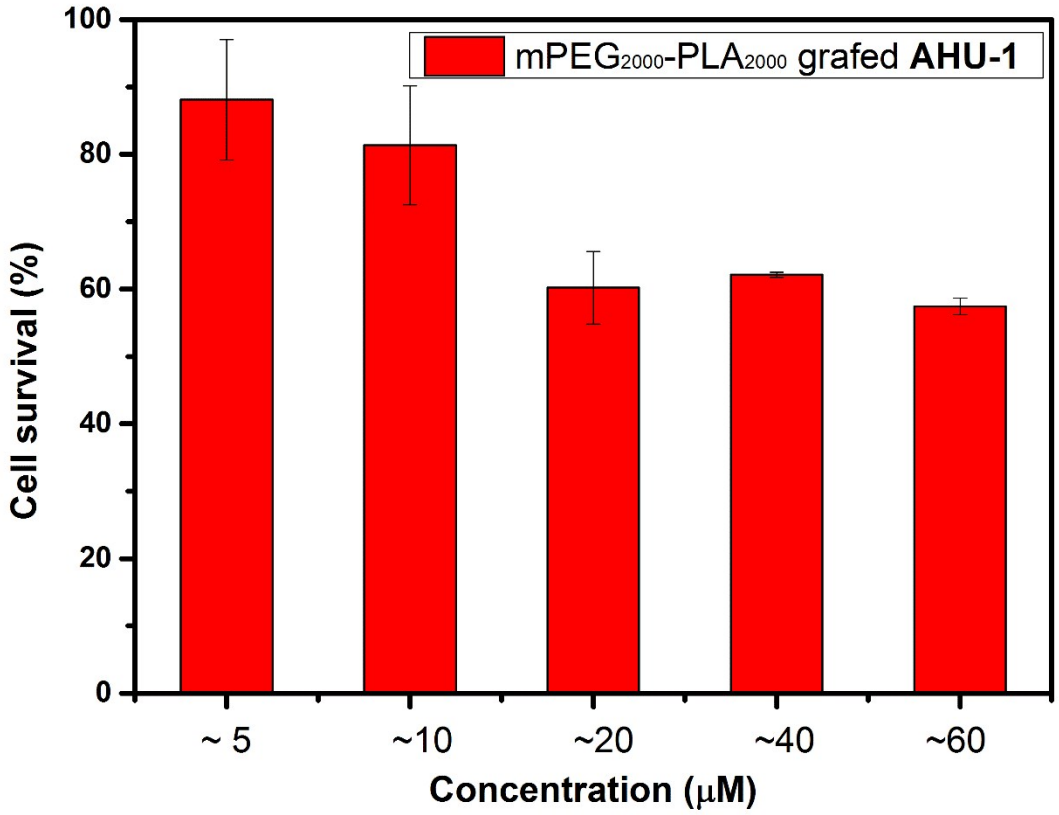

Figure S19. Cytotoxicity data results of the nanoscaled $mPEG_{2000}$-PLA_{2000} grafted **AHU-1** obtained from the MTT assay of HepG2 cells.

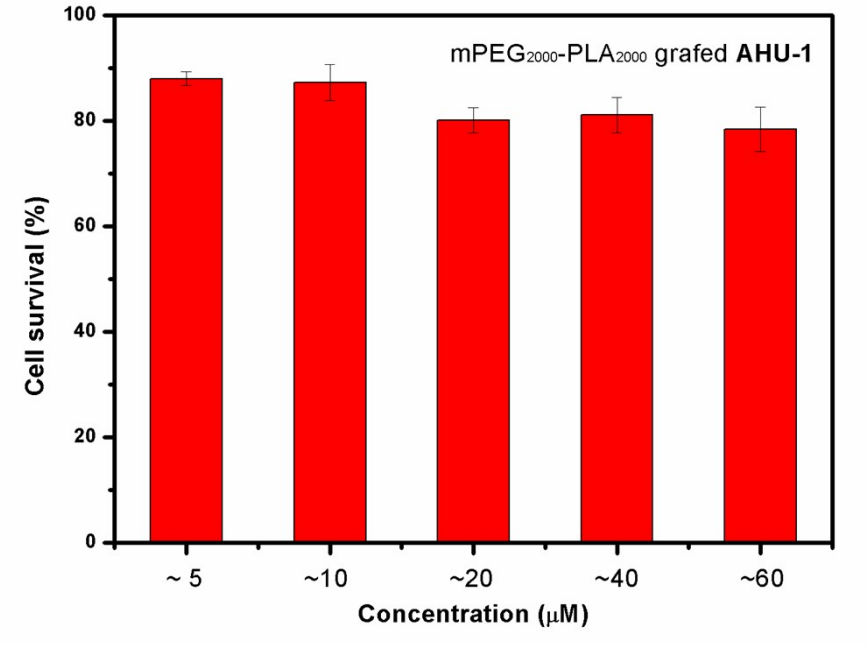

Figure S20. Cytotoxicity data results of the nanoscaled $mPEG_{2000}$-PLA_{2000} grafted **AHU-1** obtained from the MTT assay of HELF cells.

17. The imaging and imaging stability of nanoscaled AHU-1

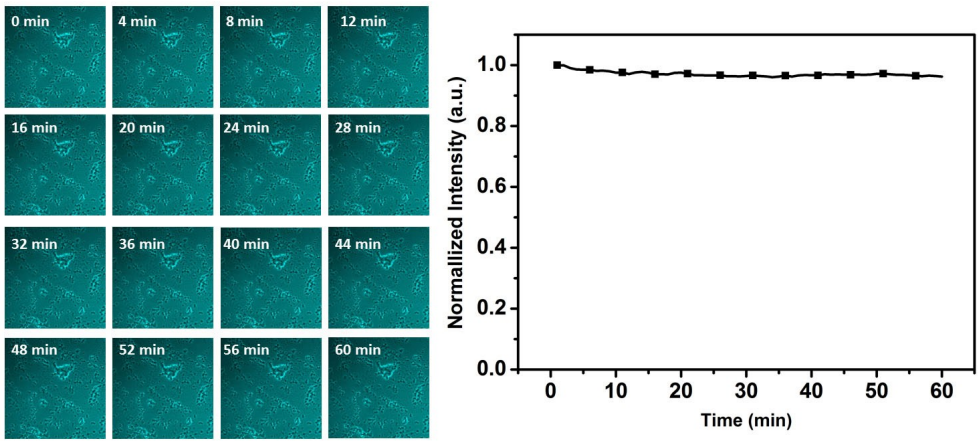

Figure S21. The imaging stability of nanoscaled **AHU-1**.

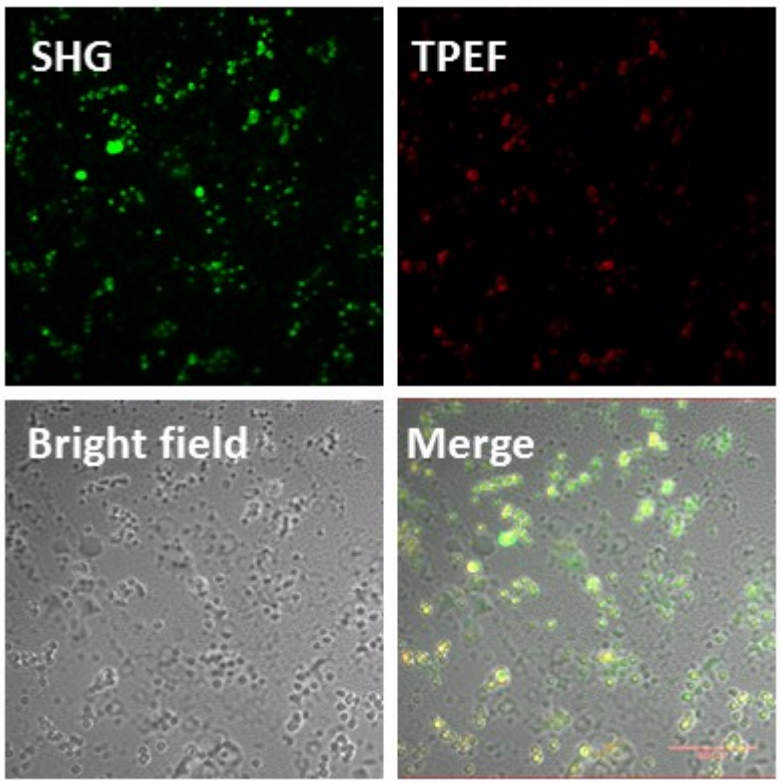

Figure S22. The imaging of AHU-1 nanocrystals.

18. Synthesis route for ligand of tpatpy

Scheme S1. The synthesis route for ligand of **tpatpy**.

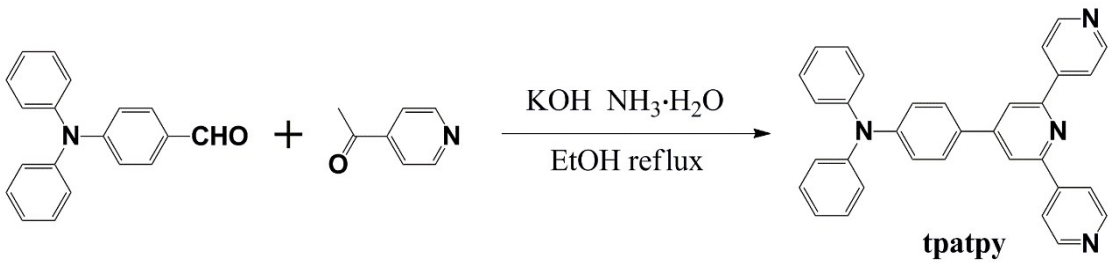

19. Crystal collection and structure refinements

Table S2. Crystal collection and structure refinements of **tpatpy**, **AHU-1**, **AHU-2** and **AHU-3**.

Identification code	**tpatpy**	**AHU-1**	**AHU-2**	**AHU-3**
Empirical formula	$C_{37}H_{40}N_4O_4$	$C_{33}H_{26}Cl_2N_4OZn$	$C_{33}H_{26}Br_2N_4OZn$	$C_{33}H_{24}I_2N_4Zn$
Formula weight	604.73	630.85	719.77	795.73
Temperature (K)	296(2)	291(2)	296(2)	296(2) K
Crystal system	Monoclinic	Orthorhombic	Orthorhombic	Orthorhombic
Wavelength (Å)	0.71073	0.71073 A	0.71073	0.71073
Space group	C2/c	$Pna2_1$	$Pna2_1$	$Pna2_1$
Unit cell dimensions (Å,°)				
a	24.68(3)	16.865(2)	16.8908(15)	16.8521(1)
b	16.725(2)	18.865(2)	18.9611(1)	19.1747(1)
c	8.173(9)	9.5230(12)	9.6680(9)	9.9703(9)
β	91.881(1)	90	90	90
Volume ($Å^3$, Z)	3371(6)	3029.8(7)	3096.4(5)	3221.7(5)
Calculated density (gcm^{-3})	1.191	1.383	1.544	1.641
F(000)	1288	1296	1440	1544
Absorption coefficient, μ/mm^{-1}	0.078	1.020	3.406	2.706
No. of reflections measured	11069	22261	22222	22166
No. of independent reflections	2949	5823	5584	5427
R_{int}	0.0430	0.0688	0.0453	0.0361
No. of formula units per unit cell ,Z	4	4	4	4
R_1, wR_2 [$I \geq 2\sigma(I)$]	0.0821 / 0.2602	0.0500 / 0.1105	0.0388 / 0.0853	0.0344 / 0.0640
R_1, wR_2 *[all data]*	0.1126 / 0.2840	0.1021 / 0.1274	0.0647 / 0.0943	0.0525 / 0.0700
GOF	1.052	0.987	0.995	1.013
Largest diff. peak and hole	0.089 / -0.087	0.260 /-0.343	0.391 / -0.386	0.640 / -0.434

(eÅ^{-3})

$^{a}R1 = \Sigma||F_o| - |F_c||/\Sigma|F_o|$, $wR_2 = [\Sigma w(F_o^2 - F_c^2)^2/\Sigma w(F_o^2)^2]^{1/2}$.

20. Selected bond lengths and angles

Table S3. Selected bond lengths (Å) and angles (°) for **tpatpy**, **AHU-1**, **AHU-2** and **AHU-3**.

AHU-1	AHU-2	AHU-3
Cl1-Zn1=2.2078(18)	Br1-Zn1= 2.3404(10)	I1-Zn1= 2.5435(8)
Cl2-Zn1= 2.2162(19)	Br2-Zn1= 2.3461(10)	I2-Zn1= 2.5436(8)
N1-Zn1 = 2.052(5)	N1-Zn1= 2.048(4)	N1-Zn1= 2.065(4)
N3-Zn1^{i}= 2.052(5)	N3-Zn1^{iii}=2.057(5)	N3-Zn1^{v}=2.046(4)
N1-Zn1-N3^{ii}= 100.28(19)	N1-Zn1-N3^{iv}=98.7(2)	N3^{vi}-Zn1-N1=97.90(19)
N1-Zn1-Cl1= 105.36(12)	N1-Zn1-Br1= 105.55(13)	N1-Zn1-I2= 110.12(14)
N3^{ii}-Zn1-Cl1=109.13(15)	N3^{iv}-Zn1-Br1=109.31(15)	N3^{vi}-Zn1-I2=106.48(13)
N1-Zn1-Cl2 = 109.56(16)	N1-Zn1-Br2= 110.69(15)	N1-Zn1-I1= 105.63(13)
N3^{ii}-Zn1-Cl2 = 104.85(14)	N3^{iv}-Zn1-Br2=105.15(14)	N3^{vi}-Zn1-I1=110.97(14)
Cl1-Zn1-Cl2 = 125.01(7)	Br1-Zn1-Br2= 124.46(4)	I2-Zn1-I1= 122.92(3)

Symmetry transformations used to generate equivalent atoms:

i -x+3/2,y-1/2,z+1/2; ii -x+3/2,y+1/2,z-1/2; iii -x+1/2,y-1/2,z+1/2; iv -x+1/2,y+1/2,z-1/2; v -x+1/2,y+1/2,z-1/2; vi -x+1/2,y-1/2,z+1/2.

Table S4. Hydrogen Bond Lengths (Å) and Bond Angles (°).

D-H···A	d(D–H)	d(H···A)	d(D···A)	<(DHA)
O(1)--H(1B)···O(2)^{a}	0.85	2.21	2.633(4)	111
O(2)--H(2A)···O(1)^{b}	0.96	2.08	2.730(4)	123
O(1)--H(1C)···N(3)^{c}	0.85	2.14	2.880(4)	146
C(5)--H(5)···Cg(2)^{d}	0.93	2.70	3.549(5)	152

Symmetry codes: (a) 3/2-x, 1/2-y, 1-z; (b) 3/2-x, -1/2+y, 3/2-z; (c) x, 1+y, z; (d) 1-x, -y, 1-z

Cg(2) equal to P5: N(3)C(16)C(15)C(14)C(17)C(18).

21. photophysical parameters of Ligand tpatpy

Table S5. Single-photon-related photophysical properties of Ligand **tpatpy** in several different solvents.

Solvents	$\lambda_{max}^{a}(\varepsilon_{max}^{b})$	λ_{max}^{c}	Φ^{d}	τ / ns^{e}

C_6H_6	293(2.97) 365(2.56)	441	0.22	3.30
CH_2Cl_2	292(3.01) 366(2.55)	486	0.21	5.55
THF	292(2.91) 364(2.57)	470	0.16	4.68
$CH_3COOC_2H_5$	290(2.72) 361(2.54)	467	0.67	4.73
C_2H_5OH	292(3.32) 368(2.63)	515	0.04	-
CH_3CN	290(2.72) 361(2.54)	515	0.14	5.18
DMF	290(3.19) 366(2.52)	510	0.71	6.19
DMSO	293(2.83) 367(2.35)	516	0.05	6.58

[a] Peak position of the longest absorption band. [b] Maximum molar absorbance in 10^4 mol^{-1} L cm^{-1}. [c] Peak position of SPEF, exited at the absorption maximum. [d] Quantum yields determined by using Quinine sulfate in 0.1 mol L^{-1} H_2SO_4 as standard.[e] The fitted fluorescence lifetime.

22. Solid fluorescent quantum yield of tpatpy, AHU-1 to AHU-3

Table S6. The solid fluorescent quantum yield of **tpatpy**, **AHU-1**, **AHU-2** and **AHU-3**.

Identification code	**tpatpy**	**AHU-1**	**AHU-2**	**AHU-3**
quantum yield	12.46%	11.03%	5.41%	1.98%

23. Molecular hyperpolarizability parameters

Table S7. Vector component of molecular hyperpolarizability the along the dipole moment direction β_μ, dipole moments of the ground states along x, y, z direction μ_x, μ_y, μ_z and total dipole moments μ_{tot} of the compounds of **tpatpy**, **AHU-1**, **AHU-2** and **AHU-3**.

Identification code	**tpatpy**	**AHU-1**	**AHU-2**	**AHU-3**
β_μ (10^{-30} *esu*)	76.0	163.9	162.1	157.7
μ_x ($10^{-30}C{\cdot}m$)	0	21.1	-23.3	26.4
μ_y (10^{-30} $C{\cdot}m$)	22.7	-34.5	-35.9	-37.7
μ_z (10^{-30} $C{\cdot}m$)	0	-52.5	-53.6	-52.8
μ_{tot} (10^{-30} $C{\cdot}m$)	22.7	66.3	68.8	70.0

24. Outlook

In this work, by using the four-coordinated distorted tetrahedral d^{10} Zn(II) ions and the conjugate D-A pull-push nonlinear organic ligand **tpatpy**, we successfully constructed a series of nonlinear optical coordination polymers (**AHU-1** to **AHU-3**) which possessed very good thermal stability, photoluminescence, second-harmonic generation and two-photon excited fluorescence. What is more, the nanoscaled **AHU-1** have been realized for three-dimentional SHG imaging of fixed mice liver and bio-imaging of living HepG2 cells. Extensive studies for the application of SHG **AHU-1** nanoparticles are under progress in our lab. For instance, SHG-based **AHU-1** might have potential for Photodynamic therapy (PDT) since the emission could serve as adjustable excitation resource for multiple photonsensitizer.

25. References

(1) Bruker AXS, SAINT Software Reference Manual, Madison, WI, 1998.

(2) G. M. Sheldrick, *Acta Crystallogr. Sect. A*, 2008, **64**, 112-122.

(3) Casassa, E. F. & Eisenberg, H. *J. Phys. Chem.*, 1961, **65**, 427-433.

(4) Albota, M., Xu, C. & Webb, W. W. *Appl. Optics*, 1998, **37**, 7352-7356.

(5) Xu, C. & Webb, W. W. *J. Opt. Soc. Am. B*, 1996, **13**, 481-491.

(6) Hong, S. Q., Chen, W., Schreyer, M. K., Hui, Y., Ming, W. W., & Wei, J., et al. *Nat. Commun.*, 2015, **6**, 7954.

(7) Frisch, M.J., Trucks, G.W., Schlegel, H.B., et al. (2010) Gaussian 09 revision C.01, Gaussian Inc. Wallingford, CT.

(8) A. D. Becke, *J. Chem. Phys.*, 1993, **98**, 5648–5652.